Molecular Sieving Membranes

International Edition: DOI: 10.1002/anie.201511340
German Edition: DOI: 10.1002/ange.201511340

Formation of Ultrathin, Continuous Metal–Organic Framework Membranes on Flexible Polymer Substrates

*Jingwei Hou, Putu D. Sutrisna, Yatao Zhang, and Vicki Chen**

Abstract: *Metal–organic framework (MOF) materials have an enormous potential in separation applications, but to realize their potential as semipermeable membranes they need to be assembled into thin continuous macroscopic films for fabrication into devices. By using a facile immersion technique, we prepared ultrathin, continuous zeolitic imidazolate framework (ZIF-8) membranes on titania-functionalized porous polymeric supports. The coherent ZIF-8 layer was surprisingly flexible and adhered well to the support, and the composite membrane could sustain bending and elongation. The membranes exhibited molecular sieving behavior, close to the theoretical permeability of ZIF-8, with hydrogen permeance up to 201 × 10^{-7} mol m^{-2} s^{-1} Pa^{-1} and an ideal H_2/CO_2 selectivity of 7:1. This approach offers significant opportunities to exploit the unique properties of MOFs in the fabrication of separation and sensing devices.*

Molecular sieving membranes are promising candidates for applications that require highly selective permeation, such as gas separation, organic solvent nanofiltration, water treatment, and chemical sensors.[1,2] The key to their successful implementation is the synthesis of a thin, but defect-free, selective layer. As a consequence of their large porosity, molecule-scale pore size, and good stability, metal–organic frameworks (MOFs) have been extensively studied for their potential as molecular sieving membranes,[3] mostly by coating them onto inorganic porous supports.[4] However such membranes are hampered considerably by their complex processing, high cost, rigidity, and brittleness. The formation of thin, continuous MOFs on porous polymeric supports has been difficult because of the lack of sufficient heterogeneous nucleation sites and adhesion.[5] Chemical modifications of the polymer surface or interfacial precipitation have been used to grow MOFs within porous substrates or as isolated crystals.[6,7] Recently, atomic-layer deposition has been applied to grow aggregates of MOF crystals directly on solid polymeric fibers for gas adsorption.[8] However, a facile approach to grow thin, continuous MOF films directly from the synthesis solution has not been available for porous flexible substrates such as polymeric membranes. Theoretically, the MOF layers can exhibit a degree of flexibility as a result of the MOF structure changing reversibly under moderate mechanical loading.[9] However, this has yet to be demonstrated in continuous, macroscopic films that act as semipermeable membranes. To achieve this, two major hurdles need to be considered: good adhesion of MOFs on flexible, porous supports and formation of a uniform, coherent film.[3]

Our group has developed a simple low-temperature hydrothermal sol-gel coating technique to deposit an ultrathin layer of TiO_2 with a controllable architecture on various polymer supports. The functionalization of the coating layer has been explored for antifouling properties, enzyme immobilization, and superhydrophobicity.[10,11] We postulated that the large surface area, nanoscale roughness, and hydrophilicity of the titania layer would promote heterogeneous crystallization on the support. Hence, we explored the formation of MOFs (specifically, ZIF-8) on APTES-functionalized (APTES = (3-aminopropyl)triethoxysilane) TiO_2-coated hollow-fiber PVDF (PVDF = polyvinylidene fluoride) membranes with a pore size of 0.05 μm (Figure 1 A). ZIF-8 is a promising candidate for the separation of olefins and hydrogen gas, water treatment, and chemical sensors[2,12] (the fabrication process is presented in Figures S1 and S2). The tunable TiO_2 coating and functionalization conditions can be used for the facile coating of a wide range of polymeric membrane structures, including flat sheets and hollow fibers. The thin and uniform TiO_2 coating layer has dual hierarchical roughness and provides OH groups for additional functionalization (Figure S3 A,B). The TiO_2 coating layer has been demonstrated to be stable under significant shear forces and harsh physical/chemical conditions.[11] Further functionalization with 2 wt% APTES forms an organosilane monolayer that provides abundant amine groups without compromising the nanoscale architecture of the TiO_2.[13]

We next deposited ZIF-8 onto PVDF membranes functionalized with APTES-titania by both preseeded growth and direct immersion in the synthesis solution. No apparent difference in the morphology of the ZIF-8 layer was observed, thus the direct immersion without preseeding was applied subsequently. We observed that a continuous polycrystalline ZIF-8 layer about 1 μm thick forms on the supporting membrane surface without any pinholes or cracks after 5 h immersion in a simple ZIF-8 synthesis mixture (Figure 1 B,C). The interface between the ZIF-8 and titania-PVDF support indicates that they are highly intercalated, which ensures stronger bonding. We postulated that the APTES-functionalized TiO_2 nanoparticles help nucleate the ZIF-8 layer

[*] Dr. J. Hou, P. D. Sutrisna, Prof. Y. Zhang, Prof. V. Chen
UNESCO Centre for Membrane Science and Technology
School of Chemical Engineering
University of New South Wales, Sydney (Australia)
E-mail: v.chen@unsw.edu.au
Prof. Y. Zhang
School of Chemical Engineering and Energy
Zhengzhou University
Zhengzhou 450001 (China)

Supporting information for this article can be found under http://dx.doi.org/10.1002/anie.201511340.

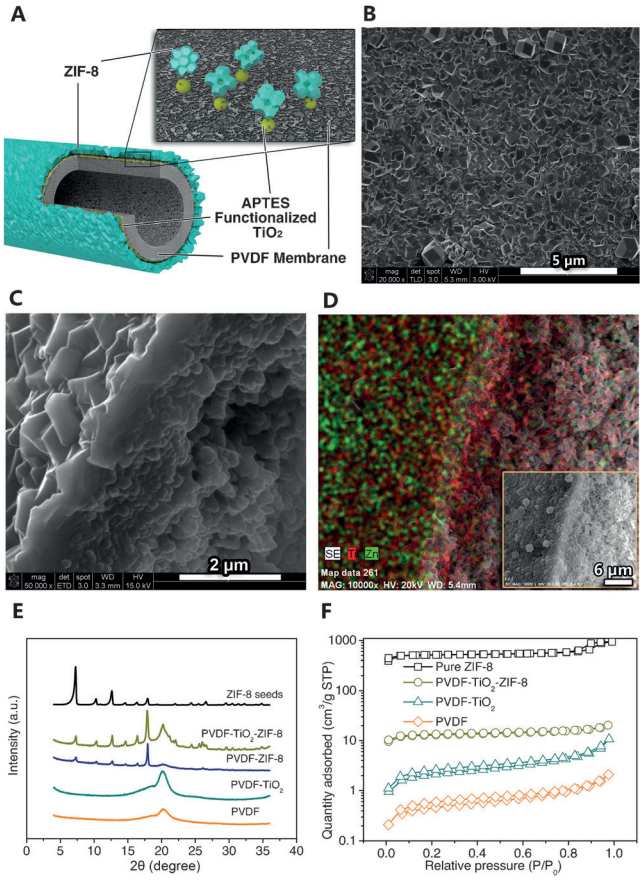

Figure 1. Description of the ZIF-8 molecular sieving membrane on a PVDF support. A) Schematic representation of the composite membrane. B,C) Surface and cross-sectional SEM images of the ZIF-8 layer. D) EDX elemental map of Ti (red) and Zn (green) (insert: reference SEM image). E,F) XRD patterns and nitrogen adsorption/desorption isotherms of the ZIF-8 crystal and the membranes with different treatment.

growth through the terminal amine groups which react with the Zn^{2+} ions to form complex metal cations.[6,14] In addition, the nanostructured titania provides a high surface area, and thus better contact and anchoring during crystallization (Table S1), thereby promoting the nucleation density of ZIF-8 on the polymer membrane surface. Such a high heterogeneous nucleation density promotes the formation of a thin and continuous ZIF-8 membrane.[15] Attempts to grow ZIF-8 on pure PVDF and TiO_2-coated PVDF (not functionalized with APTES) resulted in poorly intercalated crystals (Figure S3 C,D).

Seeking to confirm the physical, chemical, and structural properties of the ZIF-8 layer, we examined the ZIF-8 membrane by various characterization techniques. EDX (Figure 1 D) shows that the Ti is evenly distributed throughout the membrane, while there is a sharp transition of Zn between the ZIF-8 layer and the supporting membrane, thus indicating that the ZIF-8 is mainly present on the membrane surface. Thermogravimetric analysis (TGA; Figure S4) also confirms the low loading of ZIF-8, and the presence of a thin ZIF-8 layer is further supported by the ATR-FTIR results (Figure S5). The XRD patterns (Figure 1 E) suggest that the ZIF structure on the PVDF-TiO_2-ZIF-8 membrane is highly crystalline. The different relative peak intensity of the PVDF-TiO_2-ZIF-8 membrane compared with pure ZIF-8, in particular of the (222) plane ($2\theta = 18.3$), can be attributed to the preferential orientation of the crystal growth on the polymer support.[15] The gas adsorption isotherms (Figure 1 F and Figure S6), together with the results on the surface area (Table S1), are also consistent with the high adsorption area of the ZIF-8 layer.

Gas permeance is usually inversely proportional to the membrane thickness. We hypothesized that a thinner ZIF-8 layer could be obtained by controlling the ZIF-8 deposition time. However, at solution exposure times below 5 h, gas transport is mainly dominated by Knudsen diffusion (Figure 2 A and Table S2), thus indicating that the ZIF-8 layer is not continuous. The crystallization of ZIF-8 onto the functionalized PVDF membrane surface immediately resulted in the formation of nanocrystals, which served as the seeds for further crystallization. Microcrystals then formed gradually in both solution and on the membrane surface. The large particles on the membrane ensure efficient surface coverage by ZIF-8, while the fusion of nanoparticles between the large particles sealed the grain boundaries and defects, thereby forming a continuous ZIF-8 layer (Figure 2 B–F and Figure S7 A). A coherent ZIF-8 layer, formed after 5 h deposition time, clearly displayed molecular sieving properties. A further increase in the deposition time led to a thicker ZIF-8 coating and thus reduced gas permeance (Figure 2 A; Table S2 and Figure S7 B). Therefore, the ZIF-8 membrane obtained by deposition for 5 h was selected for further study. It has the highest H_2 permeance among the polymer-supported ZIF-8 molecular sieving membranes (Table S3). Our ZIF-8 membrane has superior performance over most ZIF-8 membranes supported on inorganic membranes, with the exception of the Al_2O_3-supported ZIF-8 produced by contradiffusion methods.[14] The ultrahigh H_2 permeance obtained in the present study can be attributed to the thin and activated ZIF-8 layer as well as the nanoscale surface structure of the ZIF-TiO_2 interface, thereby allowing better contact between the feed gas and the ZIF crystals.[14,16] Although the overall ZIF-8 thickness is around 1 μm, the presence of valleys between neighboring microcrystals allows much shorter distances for gas permeance (ca. 400 nm, Figure S8). On the basis of diffusivity measurements using the gas adsorption tests with ZIF-8 crystals, Zhang and coworkers estimated the ideal gas permeability through a ZIF-8 layer (H_2: 22000 Barrer, CO_2: 3300 Barrer, O_2: 2500 Barrer, N_2: 1000 Barrer, and CH_4: 270 Barrer (1 Barrer $= 10^{-10}$ cm^3(STP) cm^{-1} s^{-1} $cmHg^{-1}$).[17] Assuming the gas transport is dominated by the thinner part (400 nm) within the ZIF-8 layer, the gas permeability estimated from this present study yielded H_2: 24120 Barrer, CO_2: 3444 Barrer, O_2: 2940 Barrer, N_2: 3096 Barrer, and CH_4: 2808 Barrer. The values of H_2, CO_2, and O_2 are in good agreement with the theoretical values, while the higher permeability for N_2 and CH_4 can be attributed to the flexibility of the organic ligands on the ultrathin ZIF-8 layer, which allows larger molecules to pass through.[18] The gas separation performance easily surpasses the Robeson upper bounds (Figure S9).[19]

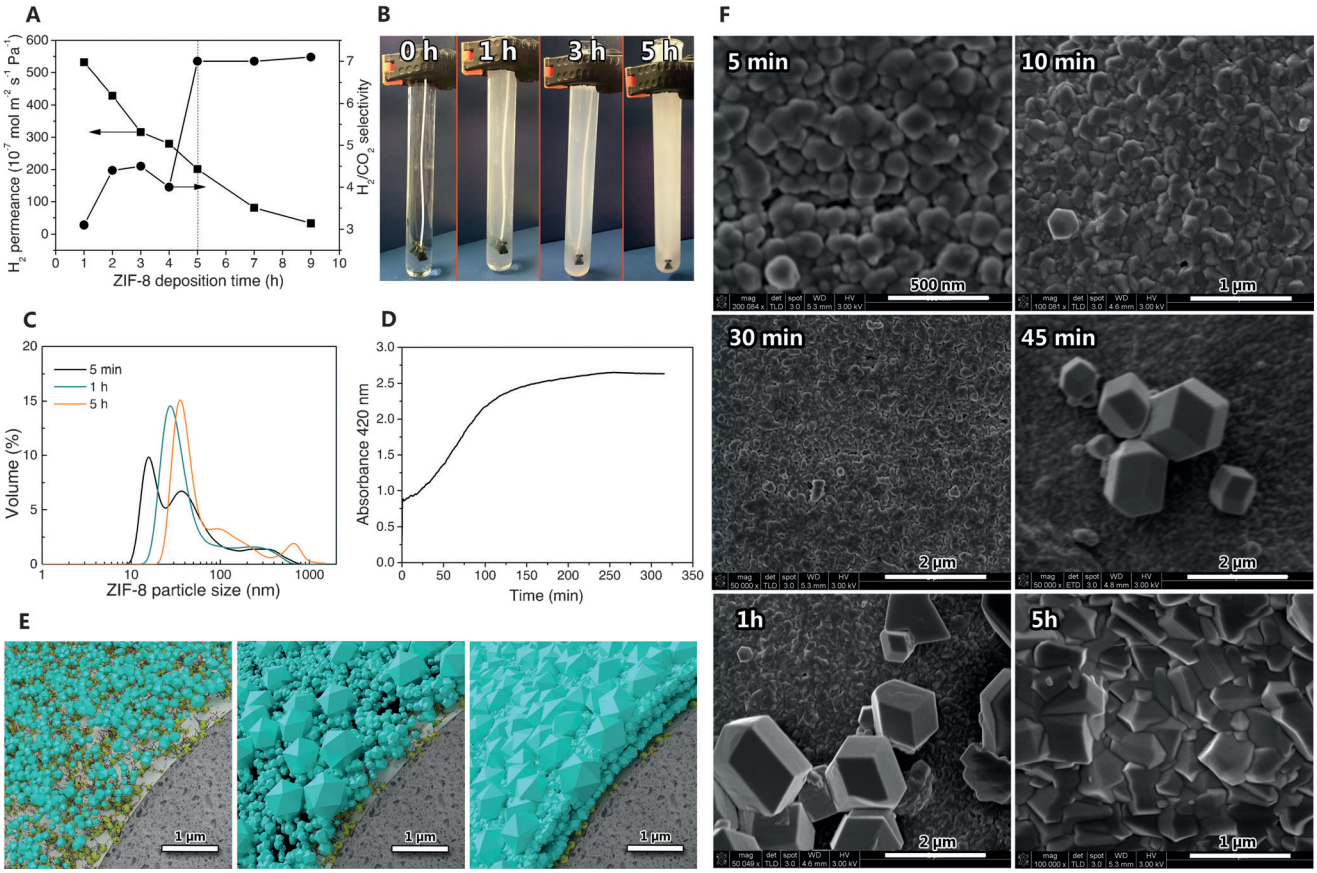

Figure 2. Gradual deposition of ZIF-8 onto the support surface. A) H_2 permeance and H_2/CO_2 ideal selectivity of membranes with different ZIF-8 deposition times. B) Photograph of the ZIF-8 deposition process. C) Change in the ZIF-8 crystal size within the deposition solution. D) Turbidity of the suspension liquid during the deposition process. E) Schematic diagram of the ZIF-8 deposition process. F) Surface SEM images of the ZIF-8 deposition process with different reaction times. Fast amorphization occurred when the nanoscale ZIF-8 was exposed to the electron beam.

For practical applications, the membrane stability under mechanical stress, long-term operation, elevated temperature, and high pressure are crucial. Tan et al. have demonstrated that the Zn-mIm-Zn linkages (mIm = methylimidazole) in ZIF-8 are more compliant and the structure has greater flexibility than conventional open-framework materials.[20] During uniaxial straining, such as stretching and compression, the flexibility is mainly provided by the reversible change in the N-Zn-N and Zn-mIm-Zn bond angles. The ZIF-8 films supported on polymer membranes could be bent up to 180° without creating visible fragmentation and tearing of the ZIF-8 layer (Figure 3A). The gas permeation results also suggest no apparent change in the gas permeation performance after bending (Figure 3B). However, the ZIF-8 layer clearly improves the tensile strength of the whole composite membrane, and it shows elastic behavior at a low elongation rate (< 3%, Figure 3C). The gas permeation tests after 3% elongation further confirms the integrity of the ZIF-8 film. The SEM images (Figure 3C) indicate the formation and growth of ZIF-8 cracks under excessive additional stress. The plastic deformation of the PVDF polymer (elongation higher than 30%) resulted in surface wrinkling for both PVDF and PVDF-TiO_2-ZIF-8 membranes. However, no detachment of the ZIF layers was observed, thus demonstrating the strong bonding between the ZIF and the support as well as the flexibility of the ZIF-8 membrane. However, ZIF-8 has a relatively low shear modulus (0.967 GPa) compared with its Young's modulus and bulk modulus (2.98 and 7.751 GPa, respectively).[20] Therefore, the shear-induced plasticity and rupture need to be avoided to ensure the integrity of the ZIF-8 layer. This study is one of the first to elucidate the mechanical properties of a continuous MOF film.

The ZIF-8 membrane performed stably for up to 30 days, but thermal treatment led to a significant loss of the permeance. The XRD pattern and the SEM images reveal loss of the crystalline phase after thermal treatment (Figure S10). ZIF-8 has very good thermal stability up to 300 °C.[21] Thus, amorphization could be caused by thermal-induced expansion of the PVDF, which imposes excessive stress on the ZIF-8 layer.[20,22] As a result, the polymer-supported ZIF-8 membrane is considered not suitable for operation at high temperatures. Furthermore, the ZIF-8 film did not collapse and fail under elevated pressures, even when the supporting membrane was severely deformed (Figure S11). To test the stability of the composite membrane against organic solvent, we prepared the flat-sheet composite membrane of ZIF-8 and soaked the membrane in dimethylacetamide (DMAc). This removed the PVDF polymer

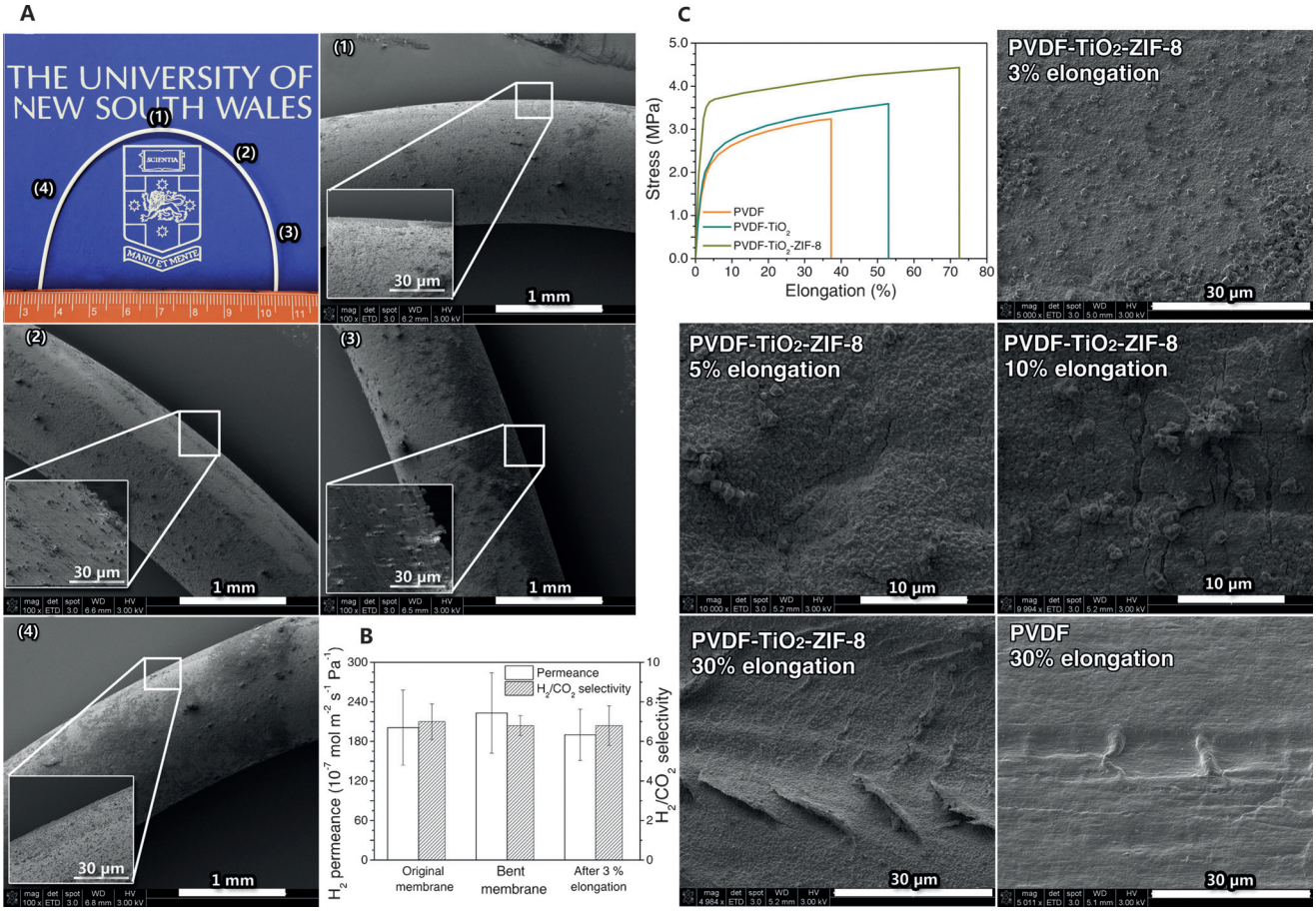

Figure 3. Behavior of the ZIF-8 membrane under different mechanical stress. A) Optical and SEM images of the bent ZIF-8 membranes. B) Performance of the ZIF-8 membrane before and after the mechanical stability test. C) Tensile testing of the membranes and the SEM images of the membrane with different levels of elongation.

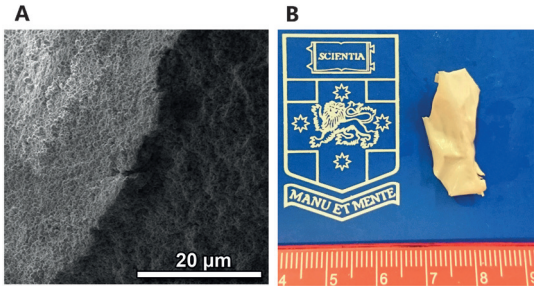

Figure 4. Flexible ZIF-8 layer on a TiO_2 exoskeleton. A) Cross-section SEM. B) Optical image of the surface.

support to leave a flexible, free-standing ZIF-8 layer on top of a highly porous TiO_2 exoskeleton, which originally encapsulated the polymer membrane structure (Figure 4 and Figure S12). This could lead to a novel route to develop an ultrathin free-standing MOF layer on a porous TiO_2 support. As a consequence of the mechanical rigidity of the TiO_2 exoskeleton under high temperature,[11] the resultant free-standing MOF layer should be able to maintain good thermal stability rather than losing its crystallinity (see Figure S10).

We also obtained a similar coherent ZIF-8 membrane on polyacrylonitrile (PAN) hollow fiber membranes (Table S4 and Figure S13). Compared with the PVDF support, the PAN-supported ZIF-8 membrane has lower permeance, which could be partially attributed to the formation of smaller pores in the support and thicker ZIF-8 layers. The PAN-based ZIF-8 composite membrane possessed comparable selectivity as the PVDF-supported membranes.

In conclusion, we reported here a facile fabrication approach to generate an ultrathin MOF membrane on a polymeric porous support. This study is one of the first to identify the mechanical flexibility of a coherent MOF film. In general, the developed MOF membrane has high permeance, good stability, and mechanical flexibility for many potential separation and sensing applications.

Acknowledgements

This work was supported by the Australian Research Council's Discovery Projects funding scheme (DP1095930, DP130104048), Australia Award Scholarship, China Scholarship Council, and UNSW Goldstar Award.

Keywords: gas separation · hollow fibers · membranes · metal–organic frameworks · molecular sieving

How to cite: *Angew. Chem. Int. Ed.* **2016**, *55*, 3947–3951
Angew. Chem. **2016**, *128*, 4015–4019

[1] a) S. Sorribas, P. Gorgojo, C. Téllez, J. Coronas, A. G. Livingston, *J. Am. Chem. Soc.* **2013**, *135*, 15201; b) R. Ameloot, F. Vermoortele, W. Vanhove, M. B. J. Roeffaers, B. F. Sels, D. E. De Vos, *Nat. Chem.* **2011**, *3*, 382.
[2] Z. Hu, Y. Chen, J. Jiang, *J. Chem. Phys.* **2011**, *134*, 134705.
[3] J. Gascon, F. Kapteijn, *Angew. Chem. Int. Ed.* **2010**, *49*, 1530; *Angew. Chem.* **2010**, *122*, 1572.
[4] J. Yao, H. Wang, *Chem. Soc. Rev.* **2014**, *43*, 4470.
[5] W. Li, Z. Yang, G. Zhang, Z. Fan, Q. Meng, C. Shen, C. Gao, *J. Mater. Chem. A* **2014**, *2*, 2110.
[6] A. Huang, H. Bux, F. Steinbach, J. Caro, *Angew. Chem. Int. Ed.* **2010**, *49*, 4958; *Angew. Chem.* **2010**, *122*, 5078.
[7] a) E. Shamsaei, Z.-X. Low, X. Lin, A. Mayahi, H. Liu, X. Zhang, J. Z. Liu, H. Wang, *Chem. Commun.* **2015**, *51*, 11474; b) W. Li, G. Zhang, C. Zhang, Q. Meng, Z. Fan, C. Gao, *Chem. Commun.* **2014**, *50*, 3214; c) A. J. Brown, N. A. Brunelli, K. Eum, F. Rashidi, J. R. Johnson, W. J. Koros, C. W. Jones, S. Nair, *Science* **2014**, *345*, 72.
[8] a) J. Zhao, M. D. Losego, P. C. Lemaire, P. S. Williams, B. Gong, S. E. Atanasov, T. M. Blevins, C. J. Oldham, H. J. Walls, S. D. Shepherd, M. A. Browe, G. W. Peterson, G. N. Parsons, *Adv. Mater. Interfaces* **2014**, *1*, 1400040; b) J. Zhao, B. Gong, W. T. Nunn, P. C. Lemaire, E. C. Stevens, F. I. Sidi, P. S. Williams, C. J. Oldham, H. J. Walls, S. D. Shepherd, M. A. Browe, G. W. Peterson, M. D. Losego, G. N. Parsons, *J. Mater. Chem. A* **2015**, *3*, 1458.
[9] J. C. Tan, A. K. Cheetham, *Chem. Soc. Rev.* **2011**, *40*, 1059.
[10] a) A. Razmjou, J. Mansouri, V. Chen, M. Lim, R. Amal, *J. Membr. Sci.* **2011**, *380*, 98; b) J. Hou, C. Ji, G. Dong, B. Xiao, Y. Ye, V. Chen, *J. Mater. Chem. A* **2015**, *3*, 17032.
[11] J. Hou, G. Dong, Y. Ye, V. Chen, *J. Membr. Sci.* **2014**, *469*, 19.
[12] G. Lu, J. T. Hupp, *J. Am. Chem. Soc.* **2010**, *132*, 7832.
[13] J. Hou, G. Dong, B. Luu, R. G. Sengpiel, Y. Ye, M. Wessling, V. Chen, *Bioresour. Technol.* **2014**, *169*, 475.
[14] Z. Xie, J. Yang, J. Wang, J. Bai, H. Yin, B. Yuan, J. Lu, Y. Zhang, L. Zhou, C. Duan, *Chem. Commun.* **2012**, *48*, 5977.
[15] S. R. Venna, M. A. Carreon, *J. Am. Chem. Soc.* **2010**, *132*, 76.
[16] M. Kanezashi, K. Yada, T. Yoshioka, T. Tsuru, *J. Am. Chem. Soc.* **2009**, *131*, 414.
[17] C. Zhang, R. P. Lively, K. Zhang, J. R. Johnson, O. Karvan, W. J. Koros, *J. Phys. Chem. Lett.* **2012**, *3*, 2130.
[18] F. Cacho-Bailo, B. Seoane, C. Téllez, J. Coronas, *J. Membr. Sci.* **2014**, *464*, 119.
[19] L. M. Robeson, *J. Membr. Sci.* **2008**, *320*, 390.
[20] J.-C. Tan, B. Civalleri, C.-C. Lin, L. Valenzano, R. Galvelis, P.-F. Chen, T. D. Bennett, C. Mellot-Draznieks, C. M. Zicovich-Wilson, A. K. Cheetham, *Phys. Rev. Lett.* **2012**, *108*, 095502.
[21] K. S. Park, Z. Ni, A. P. Côté, J. Y. Choi, R. Huang, F. J. Uribe-Romo, H. K. Chae, M. O'Keeffe, O. M. Yaghi, *Proc. Natl. Acad. Sci. USA* **2006**, *103*, 10186.
[22] V. I. Hegde, J.-C. Tan, U. V. Waghmare, A. K. Cheetham, *J. Phys. Chem. Lett.* **2013**, *4*, 3377.

Received: December 7, 2015
Published online: February 23, 2016

